

used along with barrier methods. The several published reports of other spermicides used have yielded disparate results. Pearl indices, for example, have ranged from 0 to 67 pregnancies per 100 woman-years<sup>7</sup>. This variability may reflect differences in the doses and formulations of the spermicides studied, the underlying fecundity of the study populations, lack of compliance with instructions for use of the spermicide or coital patterns. The pregnancy probabilities we observed were in the range previously accepted for users of spermicides and other barrier methods<sup>8</sup>. In our study the Pearl index was 2.3, which is acceptable for the general population of a developing country. The Drugs Controller General gave permission for this drug after complete review of preclinical and clinical data. Currently, nonoxynol-9 and benzalkonium chloride are available as spermicides, but recent studies have shown that under *in vivo* conditions nonoxynol-9 induces a proinflammatory response in vagina<sup>9</sup>. The main side-effect of spermicides is burning sensation in vagina. In our study we found only 2.34% patient complained of burning, which is very low incidence. No serious adverse events related to the spermicides occurred in our study, and the cumulative risks of the local effects evaluated in our analysis were not alarmingly high in any spermicide group. This study shows that Consap cream when used properly in indicated quantity is an effective contraceptive method. Women who do not want use oral contraceptives or intrauterine devices now have a good alternative.

1. World Population Prospects, The 2010 revision available at [http://esa.un.org/unpd/wpp/Other-Information/Press\\_Release\\_WPP2010.pdf](http://esa.un.org/unpd/wpp/Other-Information/Press_Release_WPP2010.pdf)
2. Setty, B. S., Kamboj, V. P. and Khanna, N. M., Screening of Indian plants for biological activity. Part VII. Spermicidal activity of Indian plants. *Indian J. Exp. Biol.*, 1977, **15**, 231–232.
3. Garg, S., Doncel, G., Chabra, S., Upadhyay, S. N. and Talwar, G. P., Synergistic spermicidal activity of neem seed extract, reetha saponins and quinine hydrochloride. *Contraception*, 1994, **50**, 185–190.
4. Setty, B. S., Kamboj, V. P., Garg, H. S. and Khanna, N. M., Spermicidal potential of saponins isolated from Indian medicinal plants. *Contraception*, 1976, **14**, 571–578.
5. Tiwari, P., Singh, D. and Singh, M. M., Anti-*Trichomonas* activity of *Sapindus* saponins, a candidate for development as microbicide contraceptive. *J. Antimicrob. Chemother.*, 2008, **62**, 526–534.
6. Ojha, P., Maikhuri, J. P. and Gupta, G., Effect of spermicides on *Lactobacillus acidophilus in vitro* – nonoxynol-9 vs *Sapindus* saponins. *Contraception*, 2003, **68**, 135–138.
7. Raymond, E. G., Chen, P. L. and Luoto, J., Contraceptive effectiveness and safety of five nonoxynol-9 spermicides: a randomized trial. *Obstet. Gynecol.*, 2004, **103**, 430–439.
8. Steiner, M. J., Contraceptive effectiveness: what should the counseling message be? *JAMA*, 1999, **282**, 1405–1407.
9. Patton, D. L., Kidder, G. G., Sweeney, Y. C., Rabe, L. K. and Hillier, S. L., Effects of multiple applications of benzalkonium chloride and nonoxynol-9 on the vaginal epithelium in the pigtailed macaque (*Macaca nemestrina*). *Am. J. Obstet. Gynecol.*, 1999, **180**, 1080–1087.

ACKNOWLEDGEMENTS. We thank Prof. Veena Mathur, Agra; Prof. Krishna Mukharji, Allahabad; Prof. Jayanti Kar, Gorakhpur; Dr

Kamlesh Manhans, Jammu; Prof. V. K. Singh, Kanpur and Prof. Usha Sharma, Meerut for conducting clinical trials for the Central Drug Research Institute (CDRI), Lucknow. We also thank Dr T. K. Chakraborty, Director, CDRI; Dr Nityanand and Dr V. P. Kamboj (CDRI) for their support. This study was supported by a grant from the Ministry of Health and Family Planning, New Delhi. CDRI Communication No. 8461.

Received 6 August 2012; revised accepted 7 May 2013

## Massive emissions of carcinogenic benzenoids from paddy residue burning in North India

Chinmoy Sarkar, Vinod Kumar and Vinayak Sinha\*

Indian Institute of Science Education and Research Mohali, Sector 81, S.A.S. Nagar, Manauli PO, Mohali 140 306, India

**Benzenoids are organic pollutants emitted mainly by traffic and industrial sources. Here, using a combination of on-line *in situ* PTR-MS measurements of several benzenoids and methyl cyanide (a biomass-burning tracer), satellite remote sensing data of fire counts and back trajectory of air masses at a site in Mohali, we show that massive amounts of benzenoids are released from post-harvest paddy residue burning. Two periods, one that was not influenced by paddy residue burning (period 1, 18:00–03:30 IST; 5–6 October 2012) and another which was strongly influenced by paddy residue burning (period 2, 18:00–03:30 IST; 3–4 November 2012) were chosen to assess normal and perturbed levels. Peak values of 3830 ppb CO, 100 ppb NO<sub>x</sub>, 40 ppb toluene, 16 ppb benzene, 24 ppb for sum of all C-8 benzenoids and 13 ppb for sum of all C-9 benzenoids were observed during period 2 (number of measurements in period 2 = 570) with the average enhancements in benzenoid levels being more than 300%. The ozone formation potential of benzenoids matched that of CO, with both contributing 5 ppb/h each. Such high levels of benzenoids for 1–2 months in a year aggravate smog events and can enhance cancer risks in northwestern India.**

**Keywords:** Atmospheric chemistry, benzene, cancer, methyl cyanide.

BIOMASS burning affects the environment across varied spatial and temporal scales in several regions of the world<sup>1</sup>. It contributes significantly to the global atmos-

\*For correspondence. (e-mail: vsinha@iisermohali.ac.in)

pheric budgets of gases and aerosols, perturbs regional atmospheric composition and amplifies reaction rates responsible for the formation of secondary air pollutants such as ozone and secondary organic aerosol, impairing regional air quality<sup>2</sup>. In northwestern India, large-scale burning of crop residue takes place twice a year during the post-harvest months of October–November (mainly rice) and April–May (mainly wheat)<sup>3,4</sup>. About 12,685 sq. km of paddy crop area in Punjab alone was reported to have been burnt in October 2005 (ref. 5).

Although previous crop residue burning studies in India<sup>3,6,7</sup> have focused on nutrient loss of soils and long-lived trace gases like methane, nitrous oxide, carbon dioxide and carbon monoxide, till date no study in India has investigated the impact of paddy residue burning on regional levels of reactive and carcinogenic benzenoid compounds such as benzene, toluene, xylene, ethyl benzene and trimethylbenzene. Benzenoid compounds and methyl cyanide are known to be emitted during biomass burning<sup>2</sup>. In fact, the predominant emission source of atmospheric methyl cyanide (global budget 0.4–1.0 Tg/year)<sup>8</sup> is biomass burning, a reason why it is considered an excellent chemical tracer of biomass-burning emissions<sup>8</sup>. Whereas methyl cyanide has a long atmospheric lifetime of about 9 months and health risks posed by it are unknown, benzenoid compounds collectively termed BTEX (benzene, toluene, ethyl benzene and xylene) are considered carcinogenic and mutagenic even at ambient levels of few tens of parts per billion (ppb)<sup>9</sup>. Unlike methyl cyanide for which biomass burning is the major source, traffic and solvent industry emissions are regarded as the main sources of atmospheric benzenoids<sup>10</sup>. Total global emissions of benzene, toluene and xylene are estimated to be 15 Tg/year (ref. 11). In India, the few studies of ambient BTEX levels reported in the literature (Hoque *et al.*<sup>12</sup> and references therein) are from urban sites in cities like Delhi, Mumbai and Kolkata. The analytical techniques used were offline methods based on passive or active sampling on adsorbents (with large potential for artefacts due to transfer losses) and quite slow, typically providing only highly averaged (daily or weekly level) temporal information.

Considering the large quanta of crop residue (116–289 Tg/year)<sup>3</sup> burnt every year in India, benzenoid emissions and environmental impacts therefrom could be quite significant owing to both direct health impacts (e.g. carcinogenic and mutagenic) and indirect effects (e.g. through its atmospheric reaction products participating in secondary pollutant formation). The high hydroxyl radical reactivity of benzenoids fuels photochemical production of ozone and secondary organic aerosol, resulting in intensification of smog episodes. Phenolics and cresols are the major first-generation products during atmospheric oxidation of most benzenoids. Moreover, a significant fraction of the benzenoid mass can partition to form aerosols. While benzenoids themselves are hydrophobic, their con-

version to phenolics and cresols in the atmosphere results in the formation of more polar (hence hydrophilic) aerosols that can increase the water vapour uptake by atmospheric aerosols and enhance fog formation. Recently, air pollution episodes gripped large parts of North India between 26 October and 8 November 2012, even affecting the capital Delhi<sup>13</sup>. A major factor deemed responsible for the acute smog was the transport of pollutant-laden air masses from the paddy residue-burning regions in Punjab and Haryana.

Here, we employ the combination of on-line ambient air chemical measurements (one measurement every minute) obtained by deploying a high-sensitivity proton transfer reaction mass spectrometer (PTR-MS) in tandem with the air quality station at the Indian Institute of Science Education and Research (IISER) Mohali, air mass back trajectories and satellite remote sensing data of fire events. Methyl cyanide and benzenoid compounds were measured concomitantly with carbon monoxide, nitrogen oxides and aerosol mass concentrations (PM 2.5 and PM 10) at the receptor site in Punjab (Mohali; 30.667°N, 76.729°E and 310 m amsl). Data measured on 3 November 2012 (a day that was impacted by air masses which had passed over the burning fields less than 72 h ago) and on 5 October 2012 (a day in the same season, but before crop residue burning activity had commenced), were used to quantify enhancements in ambient levels of methyl cyanide and benzenoids due to the paddy residue fires.

All the measurements were performed at the Atmospheric Chemistry Facility at IISER Mohali ([www.iisermohali.ac.in/facilities/AtmosChemfacility/index.html](http://www.iisermohali.ac.in/facilities/AtmosChemfacility/index.html)) installed on the rooftop of the Central Analytical Facility Building on the institute campus (~20 m above ground level), which is a suburban site in the northwestern Indo-Gangetic Plains (IGP) (30.667°N, 76.729°E; 310 m amsl). The wind sector spanning south to northwest (180°–315°) is mainly rural and agricultural land, and was the main fetch region observed in the periods covered by this study. The IISER Atmospheric Chemistry Facility is unique in South Asia and consists of India's first high-sensitivity PTR-MS, an on-line ambient air quality station and a meteorological station. The analytical details of the measurements are given below.

PTR-MS is a technique in which analyte volatile organic compound (VOC) molecules with a proton affinity (PA) greater than that of water vapour (PA of water 165 kcal/mol) undergo soft chemical ionization with reagent hydronium ions (H<sub>3</sub>O<sup>+</sup>) to form protonated molecular ions (with  $m/z$  = molecular ion + 1). Nitrogen, oxygen, carbon dioxide and methane have a lower PA than water vapour and do not cause interferences in the detection of the trace VOCs. The instrument at IISER Mohali is a high-sensitivity model (HS Model 11-07HS-088, Ionicon Analytik Gesellschaft, Austria). It has four main parts, namely (i) the ion source which produces a pure stream of H<sub>3</sub>O<sup>+</sup> ions (>95%) by plasma discharge of

water vapour, (ii) a reaction chamber in which ionization of VOCs takes place, (iii) a quadrupole mass analyser to separate the product ions and (iv) a secondary electron multiplier for detection and amplification of the ion signal. Use of the PTR-MS technique in diverse fields has been reviewed in detail elsewhere<sup>14,15</sup>.

To ensure proper data quality assurance, careful maintenance checks and performance characterization in terms of detection limits and sensitivities for the respective VOCs are carried out through regular calibrations. The instrument was calibrated for the measured compounds (range 0.3–20 ppbV) using a custom-ordered VOC gas standard containing methyl cyanide, benzene, toluene, *p*-xylene and 1,2,4-trimethylbenzene (Apel-Riemer Environmental, Inc., Colorado, USA), according to the protocols detailed in the works of Sinha *et al.*<sup>16,17</sup>. The instrumental background was also determined by sampling zero air. Methyl cyanide, benzene, toluene, sum of C8-aromatics (xylene and ethyl benzene) and sum of C9-aromatics (trimethylbenzene) were measured at the mass-to-charge ratios of  $m/z$  42,  $m/z$  79,  $m/z$  93,  $m/z$  107 and  $m/z$  121 respectively, in the selected ion monitoring mode. These VOC  $m/z$  identifications are in keeping with extensive validation studies from diverse ecosystems around the world<sup>15</sup>. The total uncertainties were determined to be 6.1%, 6.3%, 7.3%, 8.1% and 6.8% for methyl cyanide, benzene, toluene, xylene and trimethylbenzene respectively, calculated using the root mean square propagation of individual uncertainties like the 5% accuracy error inherent in the VOC gas standard concentration, the  $2\sigma$  instrumental precision error while measuring the compounds at 3 ppbV, and the flow uncertainty of 2% for each mass flow controller used during the calibration. Detection limits defined as the  $2\sigma$  noise while measuring at levels of  $\sim 0.3$ , are 0.1 ppb, 0.06 ppb, 0.08 ppb, 0.09 ppb and 0.09 ppb for methyl cyanide, benzene, toluene, *p*-xylene and 1,2,4-trimethylbenzene respectively.

Teflon (inner diameter 3.12 mm) was used as inlet tubing for the gas analysers which were collocated at about 20 m above ground. The inlets were protected from dust particles using teflon and nucleopore membrane particle filters (filter diameter 47 mm; pore size 5  $\mu$ m). Ambient air was drawn into the instruments continuously. The total sampling plus inlet residence time for all the instruments was < 70 s.

Carbon monoxide was measured using non-dispersive infrared (NDIR) filter correlation spectroscopy (Thermo Fisher Scientific, Model No. 48i). The 1 min data has an uncertainty and detection limit of 7% and 40 ppb respectively. This technique has been validated extensively<sup>18</sup>. For quality assurance of the dataset, zero drift calibration is done frequently (at least once every day) and span calibrations (100–1500 ppbV) are carried out at least once a month.

NO<sub>x</sub> (sum of NO and NO<sub>2</sub>) was measured using the chemiluminescence technique (Thermo Fisher Scientific,

Model No. 42i). The 1 min data has an uncertainty and detection limit of 7% and 0.05 ppb respectively. Zero drift and span calibration (five-point calibration in the range 10–50 ppbV) are carried out at least once every week and once every four weeks respectively.

PM10 and PM2.5 mass concentrations were measured by the standard  $\beta$ -attenuation technique (Thermo Fisher Scientific, Model No. 5014i Beta) that has a detection limit of < 1  $\mu$ g/m<sup>3</sup>. The instrument is calibrated at least once every 8 weeks.

The meteorological parameters such as wind speed, wind direction, solar radiation, ambient temperature and relative humidity were also measured using separate sensors (Met One Instruments Inc., Rowlett, Texas, USA).

Back trajectory ensemble calculations for air masses arriving at Mohali (30.667°N, 76.729°E) and New Delhi (28.519°N, 77.213°E; 20 m above ground level) on 5 October 2012 (18:30 IST) and on 3 November 2012 (18:30 IST) respectively, were performed using the NOAA HYSPLIT model and GDAS (Global Data Acquisition System) meteorology<sup>19</sup>. The trajectories were plotted on a map using Pan Map GIS software (Figure 1). Only those trajectories that were consistent with the terrain height of the measurement site (< 400 m amsl at Mohali and > 400 m amsl at Shimla) were considered for further analysis.

Moderate Resolution Imaging Spectroradiometer (MODIS; NASA/University of Maryland, 2002, MODIS Hotspot/Active Fire Detections Dataset, <http://maps.geog.umd.edu>) remote sensing fire count data were used to detect paddy residue burning activity in North India (including Bihar, Jharkhand, Rajasthan and Madhya Pradesh) for two 96 h periods from 2 October 2012 to 5 October 2012 and 31 October 2012 to 3 November 2012.

Figure 1 shows the MODIS fire count data (red crosses) from 2 to 5 October 2012 and 31 October 2012 to 3 November 2012. Two periods were considered. The first period (5 October 2012 18:00 IST–6 October 2012 03:30 IST; hereafter termed period 1) had no discernible influence of paddy residue burning and the second period (3 November 2012 18:00 IST–4 November 2012 03:30 IST; hereafter termed period 2) was intensely influenced by paddy residue burning as can be seen in the 72 h back trajectories for both Mohali and Delhi and the 96 h fire count data.

Period 1 measurements are representative of a period not influenced by paddy residue burning but still characterized by similar meteorology and dynamics as period 2. The back trajectories for Delhi are plotted to highlight that during period 2, the paddy residue burning emissions were also affecting Delhi and chemical perturbation of atmospheric composition in Delhi would be similar to that experienced at Mohali.

Figure 2 shows the enhancements in methyl cyanide (CH<sub>3</sub>CN), carbon monoxide (CO), sum of nitrogen dioxide and nitrogen monoxide (NO<sub>x</sub>), toluene and benzene

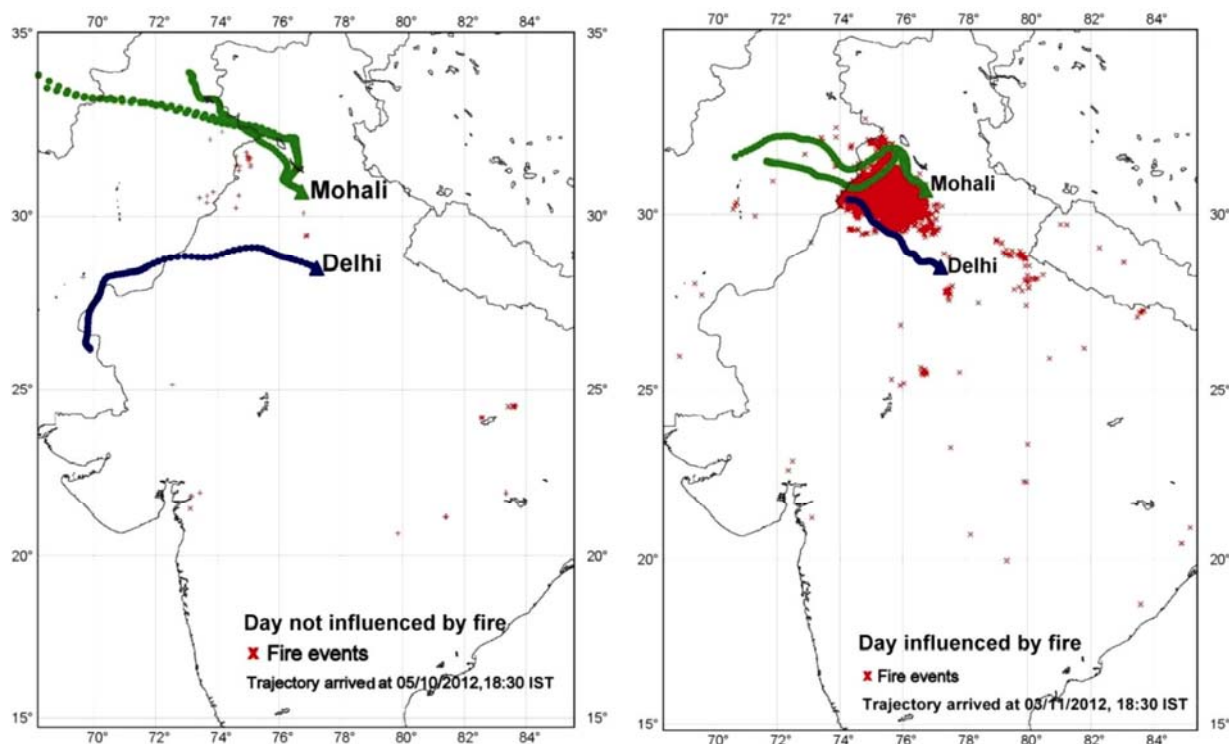


**Figure 1.** The 72 h back trajectories of air masses that arrived at 18:30 IST in Mohali and Delhi on 5 October 2012 and 3 November 2012. (Also shown are the 96 h MODIS fire count data as red markers.)

during period 2 (red triangle) relative to period 1 (black cross) between 18:00 and 03:30 IST at Mohali. During period 1, it can also be seen that the profile of the measured species is rather flat. However, the levels of all the measured species increase rapidly during period 2, from 18:30 IST till 21:30 IST and remain high until 01:00 IST. Thereafter, mixing ratios decrease and by 3:30 IST they reduce to levels typical of period 1. The increase coincides with the arrival of air masses (shaded bar) that had spent considerable time over regions where paddy residue burning was active, and enhancements in the biomass burning tracer methyl cyanide provide added confirmation. Further, the decrease in the profiles from about 3:30 IST during period 2 also coincides with a change in the direction of the back trajectory to a more northerly sector (not shown) in which paddy residue burning was absent. There seems to be a phase shift in the maxima of benzene and toluene with respect to the maxima of CO. The most likely reason for this is the manner in which the combustion process occurs. Depending on the flame temperature, oxygen availability and stage of combustion (e.g. initial stage, smouldering stage or end stage), the amount of benzene or toluene emitted relative to CO emitted from the fire would change, resulting in slightly different emission profiles.

Peak values of 100 ppb  $\text{NO}_x$ , 40 ppb toluene and 16 ppb benzene were observed for more than 30 min during period 2. Such high levels for benzene and toluene have only

been previously reported (Hoque *et al.*<sup>12</sup> and references therein) from congested traffic roads in Delhi, Mumbai and Kolkata, and demonstrate that paddy residue burning emissions can rival even the high emissions from urban traffic regionally.

The average nocturnal boundary layer (NBL) height obtained using the NOAA HYSPLIT model was 1.5 times higher in period 1 compared to period 2 (period 1<sub>NBL</sub> = 89 m; period 2<sub>NBL</sub> = 61 m). While calculating the degree of enhancement, the difference in NBL dilution was taken into account. Table 1 summarizes the results. All gas and aerosol parameters show significant enhancement (>1.5) for period 2, but, in particular, the benzenoid compounds show the highest enhancements (3.3 to 4.7). The enhancement in nitrogen oxides by a factor of 3 has strong implications for the regional levels of ozone. An excess of nitrogen monoxide relative to ozone at night would result in chemical titration of ozone mainly through the following reaction bringing down night-time ozone levels within minutes.



However, when transported to downwind sites, with the first rays of sunlight, intense ozone production would result due to the photolysis of nitrogen dioxide (at  $\lambda < 460 \text{ nm}$ ), which would further be fuelled by reactive volatile organic compounds present in the air masses.

Table 1 shows the high ozone production potential (in ppb O<sub>3</sub>/h) due to the benzenoids and CO calculated using the following equation<sup>17</sup>:

$$\text{O}_3 \text{ production potential} = (k_{(\text{VOC}_i + \text{OH})} [\text{VOC}_i]) \times [\text{OH}] \times n, \quad (2)$$

where  $k_{(\text{VOC}_i + \text{OH})}$  is the pseudo first-order rate coefficient for the reaction of species VOC<sub>*i*</sub> with OH; [VOC<sub>*i*</sub>] is the concentration of the measured VOC and  $n = 2$ .

[VOC<sub>*i*</sub>] was replaced by the measured [CO] and  $n = 1$  in eq. (2) for calculating the O<sub>3</sub> production potential due to CO.

The total ozone production potential due to just benzenoids and CO is quite high (~10 ppb/h). Note also that ozone production potential due to the measured benzenoids rivals that due to CO during period 2. Even if 50% of the high production potential (since higher O<sub>3</sub> production potential is typically accompanied by higher O<sub>3</sub> loss

potential and night-time concentrations have been used for calculating the ozone production potential) were to translate into net ozone production, the peak ozone production potential due to the benzenoids and CO chemistry would be 5 ppb/h higher. Due to increased daytime O<sub>3</sub> and NO<sub>*x*</sub>, more hydroxyl radicals would be formed (since O<sup>1</sup>D from ozone photolysis reacts with H<sub>2</sub>O and produces OH radicals) and oxidant chemistry would be amplified (as VOC + OH produces HO<sub>2</sub> and NO keeps recycling OH by converting HO<sub>2</sub> to OH), aggravating photochemical smog. Besides the primary health impact due to carcinogenic benzenoids and high ozone, significant fine-mode aerosols in the form of secondary organic aerosol would be expected to be formed, as shown in Table 1. In particular, almost 30% of the reacting benzene mass concentration could form secondary organic aerosol (Table 1). During the chemical transformations which occur in multiple steps, the more polar and hence hydrophilic water-absorbing secondary organic aerosol could coat onto the existing atmospheric particles causing them to swell up with water affecting visibility, air quality and cloud properties<sup>20</sup>.

On a regional scale in the agricultural regions and villages of northwestern India, paddy residue burning may dominate benzenoid emissions from traffic and industrial sources. The impact of crop residue burning from India on the global budget of benzenoids will require further such studies in different seasons and regions of India.

It is disconcerting to note that several paddy-growing regions of the country are also those with very high prevalence of cancer (e.g. Malwa belt in Punjab). Exposure of the population to sustained high levels of carcinogenic benzenoids in the air that they breathe for several months in a year could certainly be a contributory factor for cancer prevalence and warrants detailed multidisciplinary epidemiological and environmental studies.

It is worth mentioning that though the Ministry of Environment and Forests, Government of India stipulated new ambient air quality standards (NAAQS) in 2009 regarding permissible exposure to benzene, no standards are available for the other benzenoids. For benzene, it is stipulated that exposure to an annual average concentration of 5 µg/m<sup>3</sup> (ppb equivalent at NTP: 1.6 ppbV) (so adding up to a total exposure of 584 ppbV benzene (365 × 1.6 ppbV)) would be deemed a health hazard serious enough to warrant immediate corrective measures. If we take the average benzene concentration measured in the crop residue fire-influenced air masses of 9 ppbV during our study (based on 570 measurements), to be representative of benzene level in air masses over the crop residue burning region (a reasonable assumption as we measured at a downwind site and hence are unlikely to overestimate the value measured in the agricultural heartland where the burning occurs), and during the paddy residue burning months only, then counting the number

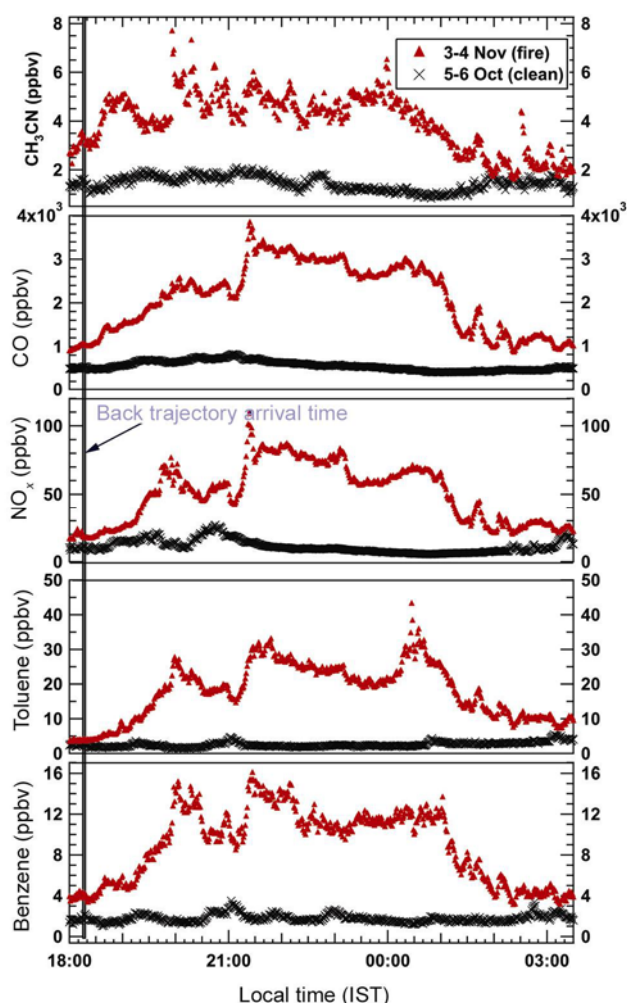


**Figure 2.** Ambient mixing ratios ( $n = 570$ ; in ppbV) of methyl cyanide, carbon monoxide, nitrogen oxides, toluene and benzene from 18:00 to 3:30 IST during period 1 (black cross; non-fire influenced) and period 2 (red triangles; fire influenced).

## RESEARCH COMMUNICATIONS

**Table 1.** Enhancement ratios, typical chemical lifetimes, ozone and secondary organic aerosol formation potentials of the measured species

Measured parameters	Air mass not influenced by crop residue burning (18:00–03:30 IST) (average $\pm$ SD)	Air mass influenced by crop residue burning (18:00–03:30 IST) (average $\pm$ SD)	Air mass influenced by crop residue burning (18:00–03:30 IST) (maximum)	Degree of enhancement*	Typical atmospheric chemical lifetime <sup>®</sup>	Ozone formation potential (ppb/h)	Secondary organic aerosol yield <sup>§</sup> (%)
Methyl cyanide* ( $m/z = 42$ )	1.1 $\pm$ 0.4	4.0 $\pm$ 1.2	7.7	3.6	268.5d	0.001	–
Benzene* ( $m/z = 79$ )	2.7 $\pm$ 0.6	8.9 $\pm$ 3.5	16.0	3.3	4.7d	0.1	27.2–29.0
Toluene* ( $m/z = 93$ )	3.8 $\pm$ 1.1	17.8 $\pm$ 8.0	43.1	4.7	1.6d	0.7	7.3–13.2
C8-Aromatics* (xylene, ethylbenzene $m/z = 107$ )	3.3 $\pm$ 0.9	13.0 $\pm$ 5.0	24.3	3.9	0.5d	1.8	2.8–8.7
C9-Aromatics* (trimethylbenzene, $m/z = 121$ )	1.9 $\pm$ 0.7	6.5 $\pm$ 2.4	12.9	3.4	0.2d	2.3	–
CO*	838.1 $\pm$ 160.9	2116.6 $\pm$ 783.9	3830.0	2.5	60d	4.9	–
NO <sub>x</sub> (NO + NO <sub>2</sub> )*	16.7 $\pm$ 7.0	50.2 $\pm$ 21.7	108.3	3	2d	–	–
PM10 <sup>#</sup>	250.0 $\pm$ 64.2	402.3 $\pm$ 123.0	587.0	1.6	–	–	–
PM2.5 <sup>#</sup>	137.1 $\pm$ 23.0	240.3 $\pm$ 62.8	320.2	1.8	–	–	–

\*Measured in ppb. <sup>#</sup>Measured in  $\mu\text{g}/\text{m}^3$ . \*Degree of enhancement is the factor by which the values are higher in period 2 compared to period 1. <sup>®</sup>Rate coefficient data were taken from Atkinson *et al.*<sup>21</sup> and  $[\text{OH}] = 3 \times 10^6$  molecules/cm<sup>3</sup> was considered; lifetime is defined as the time taken for the level to reduce to  $1/e$  of the initial value. <sup>§</sup>Secondary organic aerosol yield was at 298 K (ref. 22).

of days over which this activity occurs (at least 30 days in the year), the total exposure in this short period of time to a population inhaling such air would be 270 ppbV (30  $\times$  9 ppbV). Note that this is grim if the health risk posed by the other benzenoids and emissions during the wheat residue burning season could also be assessed. Farmers in the region burn their fields on different days depending on when the harvesting of the crop on their fields gets over. Considering the atmospheric chemical lifetimes of 4.7 days for benzene and 1.6 days for toluene (Table 1), both of which are greater than 1 day, and the ground reality that the crop residue burning activity is an almost daily occurrence during the crop residue burning season (as also evidenced by MODIS fire count data), the benzenoid release can be an even worse health risk.

Currently, the national monitoring network for benzenoid VOCs is sparse and does not even exist for methyl cyanide, for which this study reports the first ambient measurements within India. Future efforts should focus on national monitoring of ambient benzenoids using on-line analytical techniques to establish their spatial and temporal variability and constrain the contribution of its different sources for mitigation.

1. Crutzen, P. J. and Andreae, M. O., Biomass burning in the tropics: impact on atmospheric chemistry and biogeochemical cycles. *Science*, 1990, **250**, 1669–1678.
2. Andreae, M. O. and Merlet, P., Emission of trace gases and aerosols from biomass burning. *Global Biogeochem. Cycles*, 2001, **15**, 955–966.

3. Venkataraman, C. *et al.*, Emissions from open biomass burning in India: integrating the inventory approach with high-resolution Moderate Resolution Imaging Spectroradiometer (MODIS) active-fire and land cover data. *Global Biogeochem. Cycles*, 2006, **20**, GB2013 (1–12); doi:10.1029/2005GB002547.
4. Streets, D. G. *et al.*, Biomass burning in Asia: annual and seasonal estimates and atmospheric emissions. *Global Biogeochem. Cycles*, 2003, **4**, 1–20; doi:10.1029/2003GB002040.
5. Badarinath, K. V. S., Chand, T. R. K. and Prasad, V. K., Agriculture crop residue burning in the Indo-Gangetic Plains – a study using IRS-P6 AWiFS satellite data. *Curr. Sci.*, 2006, **91**, 1085–1089.
6. Gupta, P. K. *et al.*, Residue burning in rice-wheat cropping system: causes and implications. *Curr. Sci.*, 2004, **87**, 1713–1717.
7. Sahai, S. *et al.*, A study for development of emission factors for trace gases and carbonaceous particulate species from *in situ* burning of wheat straw in agricultural fields in India. *Atmos. Environ.*, 2007, **41**, 9173–9186.
8. Holzinger, R. *et al.*, Biomass burning as a source of formaldehyde, acetaldehyde, methanol, acetone, acetonitrile, and hydrogen cyanide. *Geophys. Res. Lett.*, 1999, **26**, 1161–1164.
9. WHO, *WHO Guidelines for Indoor Air Quality: Selected Pollutants* (ed. Theakston, F.), World Health Organization: WHO Regional Office for Europe, Copenhagen, Denmark, 2010, pp. 1–454.
10. Rasmussen, R. A. and Khalil, M. A. K., Atmospheric benzene and toluene. *Geophys. Res. Lett.*, 1983, **10**, 1096–1099.
11. Olivier, J. G. J. *et al.*, A set of global emission inventories of greenhouse gases and ozone depleting substances for all anthropogenic and natural sources on a per country basis and on 1° by 1° grid. In Description of EDGAR version 2.01996. National Institute of Public Health and Environment, Bilthoven, The Netherlands, 1996, pp. 66–71.
12. Hoque, R. R. *et al.*, Spatial and temporal variation of BTEX in the urban atmosphere of Delhi, India. *Sci. Total Environ.*, 2008, **392**, 30–40.

13. Singh, D., Centre terms smog as extreme pollution. In *Hindustan Times*, 1 December 2012, New Delhi.
14. Blake, R. S., Monks, P. S. and Ellis, A. M., Proton-transfer reaction mass spectrometry. *Chem. Rev.*, 2009, **109**, 861–896.
15. de Gouw, J. and Warneke, C., Measurements of volatile organic compounds in the earth's atmosphere using proton-transfer-reaction mass spectrometry. *Mass Spectrom. Rev.*, 2007, **26**, 223–257.
16. Sinha, V. *et al.*, The effect of relative humidity on the detection of pyrrole by PTR-MS for OH reactivity measurements. *Int. J. Mass Spectrom.*, 2009, **282**, 108–111.
17. Sinha, V. *et al.*, Constraints on instantaneous ozone production rates and regimes during DOMINO derived using *in situ* OH reactivity measurements. *Atmos. Chem. Phys.*, 2012, **12**, 7269–7283.
18. de Gouw, J. A. *et al.*, Emission and chemistry of organic carbon in the gas and aerosol phase at a sub-urban site near Mexico City in March 2006 during the MILAGRO study. *Atmos. Chem. Phys.*, 2009, **9**, 3425–3442.
19. Draxler, R. R. and Rolph, G. D., HYSPLIT – Hybrid Single Particle Lagrangian Integrated Trajectory Model. Model access via NOAA ARL READY website (<http://ready.arl.noaa.gov/HYSPLIT.php>), NOAA Air Resources Laboratory, Silver Spring, MD, USA, 2011.
20. Rosenfeld, D. *et al.*, Flood or drought: how do aerosols affect precipitation? *Science*, 2008, **321**, 1309–1313.
21. Atkinson, R. *et al.*, Evaluated kinetic and photochemical data for atmospheric chemistry: volume I – gas phase reactions of O<sub>x</sub>, HO<sub>x</sub>, NO<sub>x</sub> and SO<sub>x</sub> species. *Atmos. Chem. Phys.*, 2004, **4**, 1461–1738.
22. Ng, N. L. *et al.*, Secondary organic aerosol formation from m-xylene, toluene and benzene. *Atmos. Chem. Phys.*, 2007, **7**, 3909–3922.

ACKNOWLEDGEMENTS. We thank IISER Mohali and MHRD, India for institutional support and funding. C.S. and V.K. thank the Max Planck–DST India Partner Group and DST-INSPIRE scheme for student fellowships respectively. We also thank the NOAA Air Resources Laboratory for provision of the HYSPLIT transport and dispersion model.

Received 9 January 2013; revised accepted 8 April 2013

## Interpretation of coastal morphodynamics of Subarnarekha estuary using integrated cartographic and field techniques

Sabyasachi Maiti\*

Department of Geology, Presidency University, 86/1 College Street, Kolkata 700 073, India

**Cartographic techniques are frequently applied for coastal mapping, but their application for the study of coastal morphodynamics is unpopular, as they only give limited parameters like plan-view, geometry, area–length measurement and lithology. On the other**

**hand, detailed study of morphodynamics requires extra information like depthwise variation in lithology and absolute dating. Since both these techniques are expensive, cartographic techniques can be cost-effective supplementary. In the present study, morphodynamic history of Subarnarekha estuary from 7000 years BP has been interpreted applying data from cartographic techniques along with shallow wells, <sup>14</sup>C-dating and literature survey. Geomorphologic features of the coastal plain were identified in the order of hierarchy, viz. chenier plain (first order); beach ridge complex, spit complex, chenier complexes (second order); cheniers (third order); and simplest ridge, spit, washover beach (fourth order). Following this field-investigated geological history of river dynamics (both Ganges and Subarnarekha) and sea-level changes identified by earlier researchers were merged with cartographically observed features. The studied ridge chronology provides six sequences of chenier complex development agewise, whereas geometry of spit complexes suggests chronological conversion of Subarnarekha estuary from initial wave-dominated to tide-dominated flow.**

**Keywords:** Cartographic techniques, coastal morphodynamics, chenier complex, geomorphological hierarchy.

CARTOGRAPHIC techniques are popular for regional-scale mapping of any natural phenomenon or resource. The technique proves its effectiveness in decadal coastal change studies<sup>1–3</sup>. Understanding past mechanism of coastal dynamics on a regional scale is significant for hydrocarbon exploration. Such knowledge is broadly described under the studies on coastal morphodynamics. However, cartographic technique is unpopular, because this branch of science got limited scope to provide information, such as depthwise detailing of lithology, absolute age, etc. The present study shows the effectiveness of cartographic techniques by involving data from a few shallow wells and radiometric dating. The study also illustrates 7000 years past history of geomorphologic development of a coast. The coast being susceptible to environmental changes, indeed documents several centennial phenomena of gradual changes in climate, associated sea-level changes and fluctuating characters of estuaries. Therefore, through a study of coastal morphodynamics, one can interpret palaeoclimate and many past geological consequences. In the present study, Subarnarekha estuary situated in the Midnapur–Balasore coast has been considered for detailed understanding of coastal morphodynamics.

The Midnapur–Balasore coastal plain extends over 113.5 km length from Panchpara River (Odisha) to Rasulpur River (West Bengal), and also extends inland from the shoreline for 18 km. The coordinates for the area are 87°08'44"E, 21°49'12"N to 87°55'56"E, 21°31'58.82"N. The chenier complex of Subarnarekha also follows similar extension covering the whole coastal plain. The complex consists of a series of low linear hummocks of

\*e-mail: s.maiti@yahoo.co.uk